



Site-Specific Nanofabrication of Multiferroic Double-Layer Heterostructures

Undergraduate Researcher
Ken D'Aquila, Northwestern University

Faculty Adviser Mentor
Vinayak Dravid
Department of Materials Science and Engineering, Northwestern University

Graduate Student Mentor
Zixiao Pan
Department of Materials Science and Engineering, Northwestern University

Abstract

Two-phase multiferroic nanostructures have the potential to display magnetoelectricity (ME) through interphase mechanical coupling. Nanoscale ME-based technology may lead to the next generation of computer memory. In this research, soft electron beam lithography (soft-eBL) was used to fabricate submicron-sized structures of cobalt ferrite (magnetostrictive) and barium titanate (piezoelectric) as bottom and top layers, respectively. Silicon and magnesium oxide [100] substrates were used, and the MgO substrate produced structures with a well-defined faceted appearance after annealing. Geometric characterization was performed with scanning electron microscopy (SEM) and atomic force microscopy (AFM). Magnetic force microscopy (MFM) was also used to observe the magnetic orientation of the cobalt ferrite layer on MgO.

Introduction

Materials that can be ferromagnetic and ferroelectric simultaneously are called multiferroic. A promising property of multiferroic materials is magnetoelectricity. The magnetoelectric effect means that applying an external magnetic field induces an electric field from the material, and vice versa. Either a single-phase material or material system can produce this effect. Understanding the nature of ME is important not only for basic science but also for applications such as next-generation computer memory.

Recent experiments reported in the literature suggest that the ME effect is most observable in nanoscale composite structures. A two-phase composite system generates ME through mechanical coupling. One phase is magnetostrictive and the other phase is piezoelectric. A magnetic field causes the magnetostrictive layer to slightly change size. The piezoelectric phase, mechanically bonded, must also change size; in doing so, it generates an electric field. Because this system relies on mechanical surface coupling, it is expected that nanostructured composites will be advantageous due to their large interphase surface areas.

There are ceramic materials known to have the necessary magnetic and electrical properties for making these

composite structures. For example, barium titanate (BaTiO_3 or BTO) is piezoelectric and ferroelectric, while cobalt ferrite (CoFe_2O_4 or CFO) is magnetostrictive and ferromagnetic. Unfortunately, the high melting temperature and need for single-crystal structures makes a top-down nanofabrication approach too difficult.

Further study of the magnetoelectric effect requires a bottom-up nanofabrication approach that can manipulate the needed functional ceramics (BTO and CFO) and position these materials with nanoprecision into a suitable geometry for characterization.

Background

As early as 1894, researchers were hypothesizing that a magnetoelectric effect was possible.¹ Since then much experimental work on ME materials has been performed.

An important discovery was that two-phase ME composites work better than single-phase material. According to Ryu (2002), the ME effect in composites can be a hundred times stronger.³ The ME composite works through a mechanical coupling between a piezoelectric phase and magnetostrictive phase. Ryu constructed a two-layer thin film of

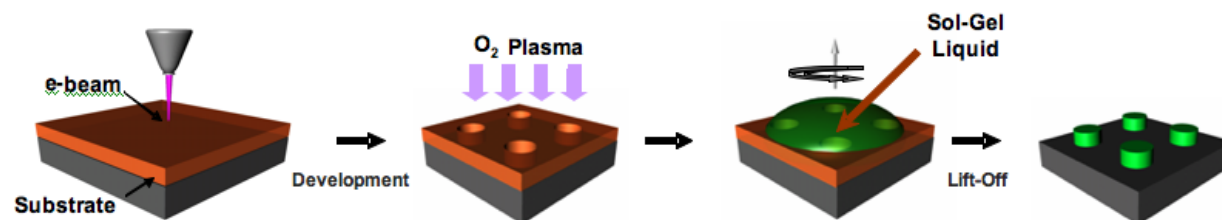


Figure 1: Overview of soft electron beam lithography approach for single-layer fabrication.

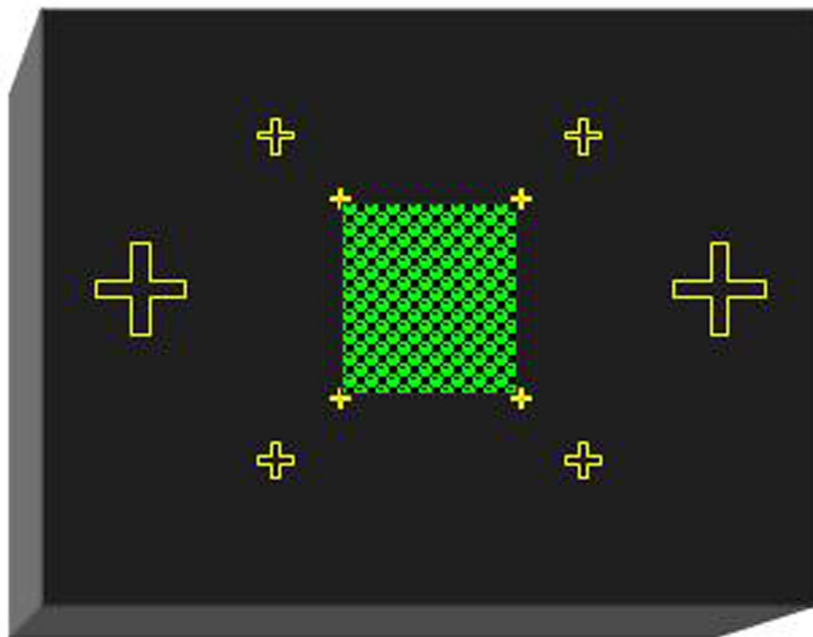


Figure 2: Schematic of alignment markers (yellow) and the patterned area (green).

piezoelectric lead zirconate titanate (PZT) and magnetostrictive Terfenol-D. Applying a magnetic field, measurements of electric polarization were obtained, and an analysis of layer thickness was performed that indicated a thinner PZT layer is preferred for higher electric polarization.

A geometrical development proposed by Zheng (2004), and confirmed by Liu's thermodynamic theory (2005), was that having magnetostrictive nanopillars vertically embedded in a piezoelectric matrix generates better ME coupling than that generated in the two-layer geometry used by Ryu.^{2,4} This complicated geometry was self-assembled using a pulsed laser deposition technique. Zheng used cobalt ferrite (CFO) and

BTO as magnetostrictive and piezoelectric materials, respectively. The similar lattice parameters of these two materials allow epitaxial bonding and thus good mechanical coupling.

Approach

The primary goal of this research was to fabricate an array of submicron-sized two-layer heterostructures composed of a CFO bottom layer and a piezoelectric BTO top layer. Electron beam lithography (eBL) was used with positive PMMA/copolymer resist to make the array pattern, and sol gels were used as liquid precursors to the ceramic layers.

Secondary goals were to increase the pattern density (more two-layered heterostructures, each smaller in size) and to characterize the structures' geometric properties and magnetic properties.

The major fabrication challenges were to build flat, smooth layers at the proper thickness, to align the layers, and to prepare epitaxial interfaces that produce correct crystallographic orientation.

The heterostructure layers were built using a three-step soft eBL approach including polymer resist spin coating, eBL, and sol deposition. A bottom layer of MicroChem PMMA/8.5% MMA referred to as "copolymer," and a top layer of 950 PMMA were spin-coated on to a thickness of about 150 nm. A scanning electron microscope (SEM) operated at 30 kV with an area dose of 300 nC/mm² was used. The polymer at the exposed "disk-shaped" regions was developed along with 1:3 methyl isobutyl ketone/isopropyl alcohol (MIBK/IPA) and then filled in with CFO sol. After the sol was allowed to form a gel, the polymer layer and excess sol were lifted off to leave the array of CFO disks. The high resolution and good registry of eBL, combined with the easy low-energy manipulation of sol ceramic precursor, make this submicron fabrication approach versatile both geometrically and for different materials. The entire process was repeated to generate the second layer, BTO.

The challenge of alignment of the two layers was resolved using three progressively smaller sizes of cross-shaped metallic markers. The markers were patterned by eBL on PMMA/copolymer and formed by sputter-coating 3 nm of Ti and 80 nm of Au. The largest markers were used to visually locate the pattern area. A CAD file then scanned the

smaller markers and simultaneously displayed the corners of the intended pattern area. This permitted the intended pattern area to be adjusted precisely within the four marker corners, ensuring good layer alignment.

Preparing single-crystal structures and epitaxial interfaces depends on the choice of substrate and the post-patterning anneal. Two substrates were explored, silicon and annealed magnesium oxide [100]. The silicon substrate was used while working out the eBL, spin-coating, and other parameters. Because of the suitable lattice parameter and crystallographic orientation of the preannealed MgO, this substrate served as a template for the ceramic layers to bond with the same [100] crystallographic orientation. The MgO samples, once patterned with CFO structures, were then annealed (1000° C, 6 hr) so that the CFO-MgO interface would be epitaxial, the CFO structure would become a single crystal, and a good flat facet would be available for the top BTO layer to bond.

Atomic force microscopy (AFM) and SEM were used to characterize the structures. Environmental scanning electron microscopy (ESEM) with 1.5 torr water vapor was used to image the insulating MgO samples. Magnetic force microscopy (MFM) was used to test the ferromagnetic property of CFO on MgO prior to constructing the top BTO layer.

Results and Discussion

Silicon

Three trials were conducted on the fabricated two-layer nanostructures on silicon substrate. The first trial's results are shown in Figure 3. In Figure 3A, the optical image confirms that a large array pattern was made. Figure 3B's SEM

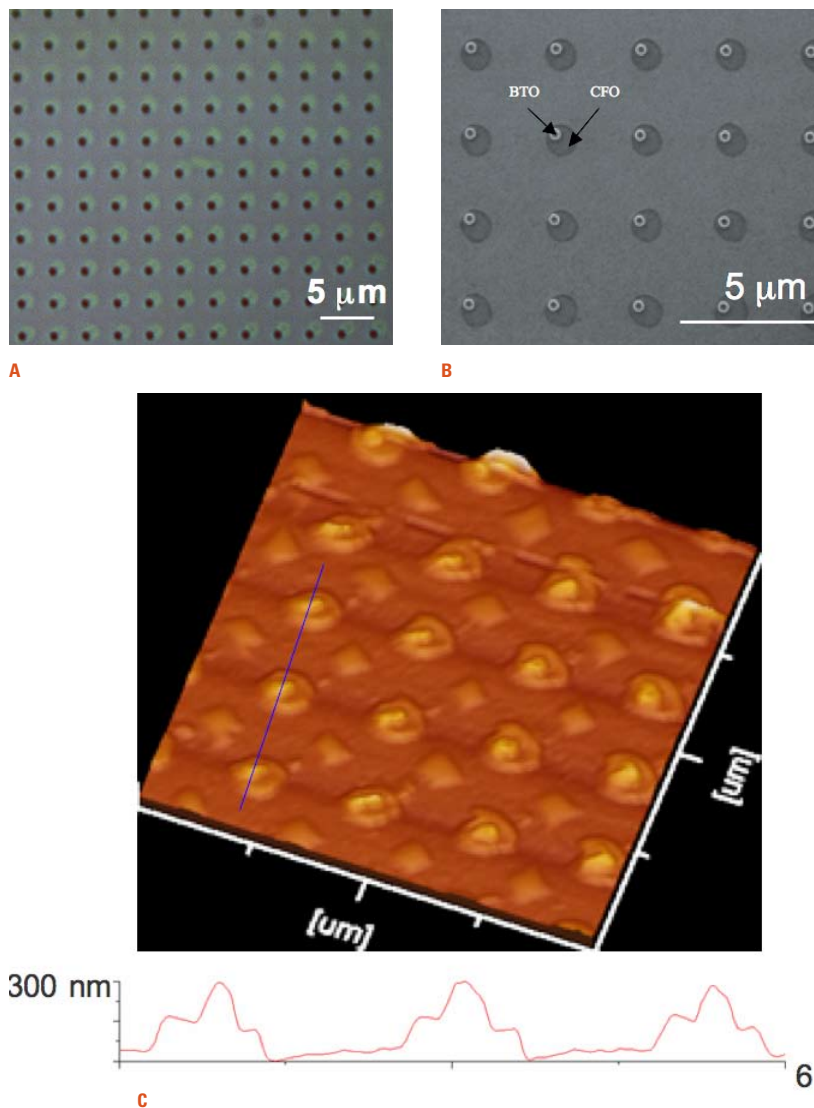


Figure 3: Unaligned double-layer nanostructures on silicon. (A) Optical image. (B) SEM image. (C) tapping mode AFM image showing the 3D construction of a 4x4 array.

Site-Specific Nanofabrication of Multiferroic Double-Layer Heterostructures (continued)

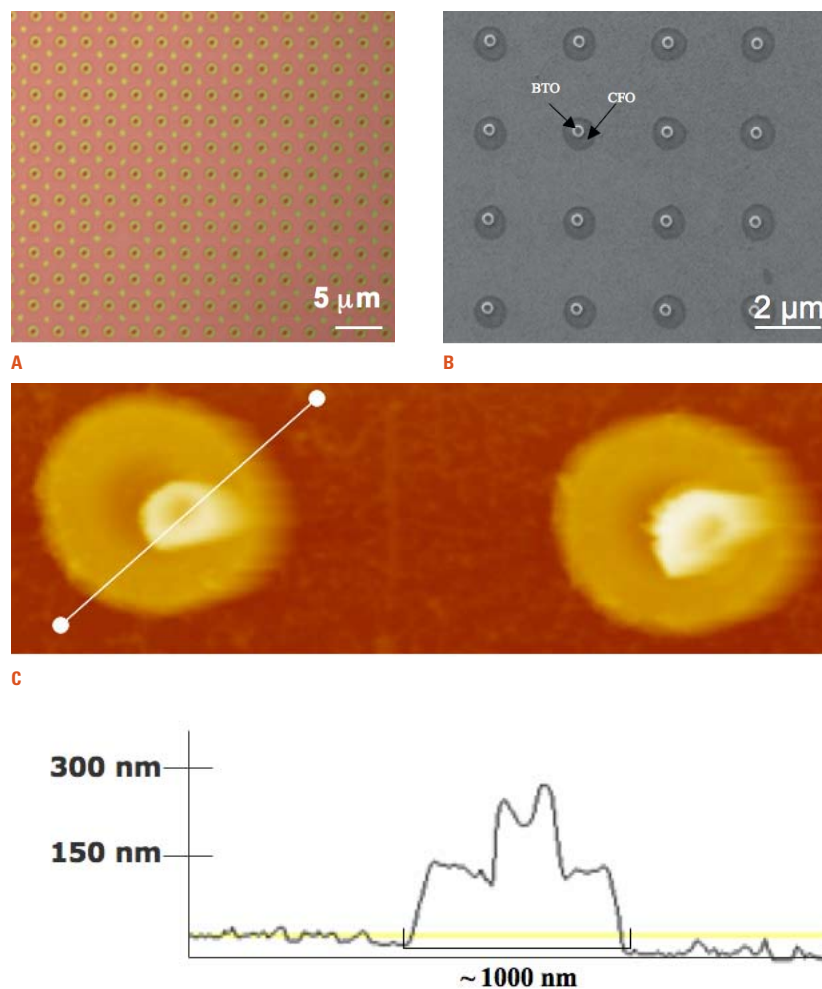


Figure 4: Aligned double-layer nanostructures on silicon. (A) Optical image. (B) SEM image. (C) tapping mode AFM image.

image indicates that each structure has the correct diameter ($\sim 1 \mu\text{m}$ bottom, $\sim 500 \text{ nm}$ top). Figure 3C's AFM results show that the height ($\sim 150 \text{ nm}$ each layer) corresponds well with the PMMA thickness from *e*BL fabrication. However, it is clear that top and bottom layer alignment is not ideal.

The second nanofabrication trial on silicon corrected the alignment problem in two ways. First, a different and more linear alignment marker scheme was adopted to reduce the stage movement distance during alignment. Second, the alignment CAD file was combined with the patterning file to reduce drift time. Figure 4 shows the corrected structures.

The third trial showcases some of soft-*e*BL's versatility. Each structure's dimension was reduced almost in half ($\sim 500 \text{ nm}$ bottom layer, $\sim 200 \text{ nm}$ top layer) by simply changing the *e*BL CAD file (see Figure 7). Soft-*e*BL has an advantage over other thin film-based methods because it can create a variety of three-dimensional structures of different sizes.

Magnesium Oxide [100]

Single-layer structures were fabricated on the MgO substrate with a size of $\sim 400 \text{ nm}$ and height of $\sim 100 \text{ nm}$. Due to time constraints, the second-layer fabrication was not completed for structures on MgO. However, Figure 6 shows AFM images of what the MgO substrate and high-temperature annealing can accomplish. Each structure takes on a "truncated pyramid" equilibrium shape that is consistent with the Wulff Construction for $m\bar{3}m$ point groups. There is also uniform facet orientation with respect to the substrate: (100) on the top and (111) for each of the sloping sides. While not yet completely

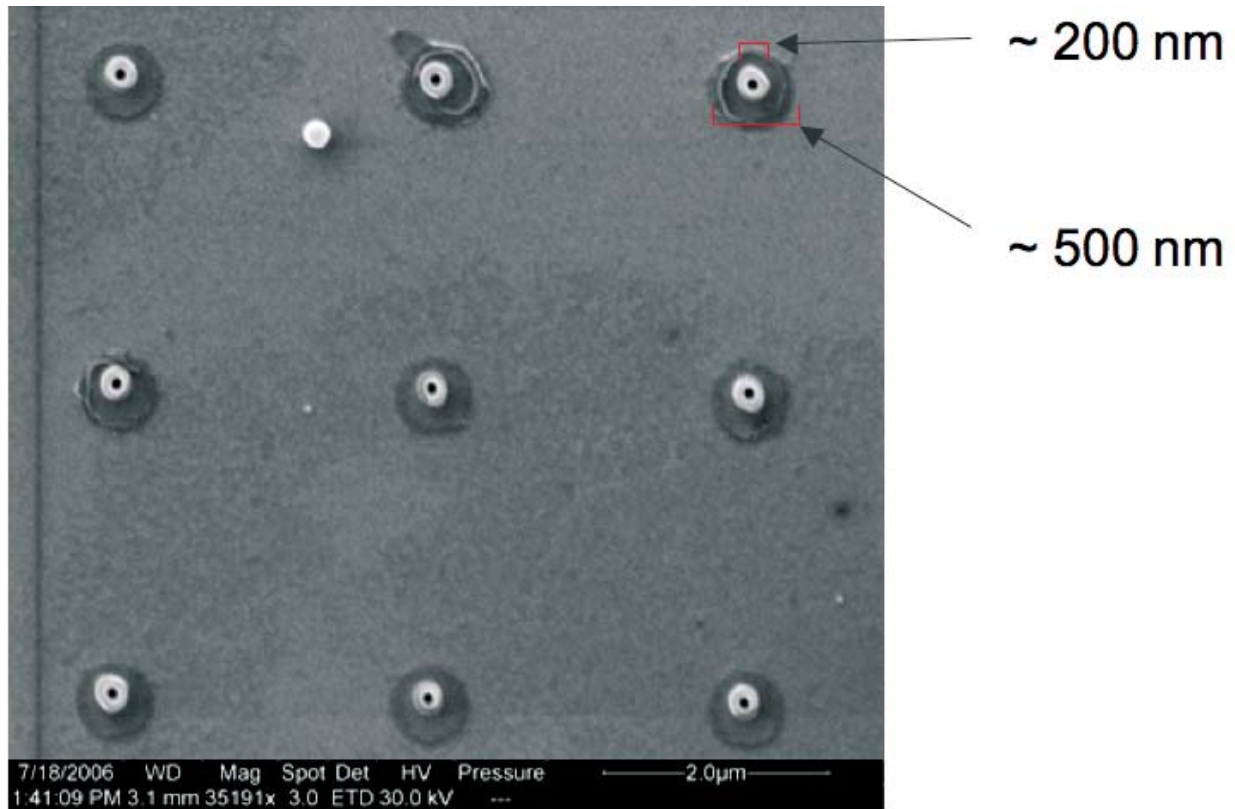


Figure 5: SEM image of CF0 (bottom). BTO nanostructures on silicon (top).

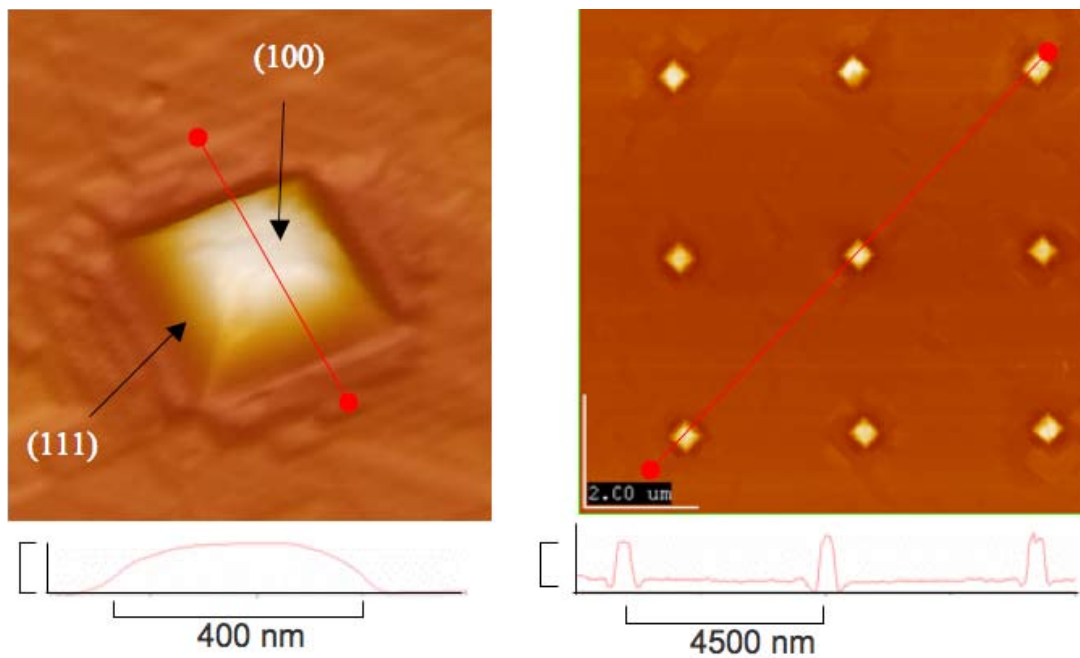


Figure 6: AFM images of CFO nanostructures on MgO (100).

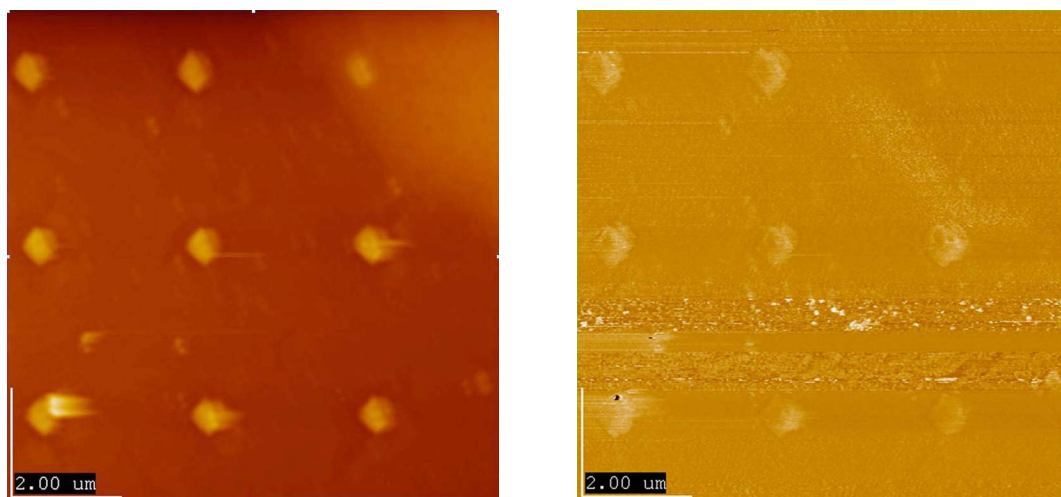


Figure 7: AFM topographic image (left) and MFM phase image (right) of CFO nanostructures on MgO (100).

conclusive, these geometric results suggest that the “microstructure” of each two-layer structure is well controlled.

MFM also signaled that that well-orientated crystallography was achieved. [100] is a direction of magnetic anisotropy in the CFO bottom layer, so getting ferromagnetism normal to the surface suggests correct crystallographic directionality. The sample was magnetized with 0.3 T, and a magnetic AFM tip was used to detect magnetic regions. The results shown in Figure 7 confirm the ferromagnetic property of CFO.

Conclusion

Great versatility, registry, and precision make soft-*e*BL a very useful nanofabrication approach. Using soft-*e*BL, functional ceramic oxides have been successfully patterned in a two-layer nanoscale geometry on silicon. The approach was also used to pattern single-layer nanostructures on MgO with a well-defined faceted morphology. All the nanostructures were geometrically characterized with SEM and AFM.

Future work includes utilizing the flat top facet of the CFO nanostructures on MgO as a based on which to build a BTO top layer; characterizing these two-layer heterostructures with transmission electron microscopy (TEM) to determine chemical composition and epitaxial interfaces (sample preparation could be facilitated by fabricating the structures on a pre-made electron transparent “window”; and developing a method to test the ME effect.

References

- (1) Curie, P. J. *Physique*, **1894**, *3*, 393.
- (2) Liu, G. et. al. *J. Phys. D: Appl. Phys.* **2005**, *38*, 2321–2326.
- (3) Ryu, J.; et al. *J. Electroceramics* **2002**, *8*, 107–119.
- (4) Zheng, H.; et al. *Science* **2004**, *303*, 661.